SOME PROPERTIES OF METASTABLE STATES OF WATER

A.N. Nevzorov

*Central Aerological Observatory, Rosgidromet, 3 Pervomayskaya Street, Dolgoprudny,
Moscow Oblast 141700, Russia*

(E-mail: an.nevzorov@mtu-net.ru)

A number of new conclusions on properties of H_2O modifications metastable with respect to the transition into crystalline ice at $T < 0°C$ were obtained. Such modifications are supercooled ordinary water (water-1) and amorphous water (A-water). This study was initiated by new data on the microphysical structure of atmospheric cold clouds (CCc). Based on the new and previously known experimental data, the concepts on the nature and properties of water amorphous condensate were corrected and complemented. It was substantiated that the optical glory phenomenon on CCs is formed as a bow of sunlight scattering by A-water droplets with a refractive index of ~ 1.8. The molecular mechanism of frontal crystallization of the metastable form of water, which explains the observed effects of water freezing, was considered.

1. Introduction

A significant number of papers, first of which was published in the middle of the nineteenth century, were devoted to the study of unfrozen water properties at temperatures below 0°C. Modern concepts were formed mostly to the 1970–80s due to the progress achieved in methods for studying the internal structure and macrophysical properties of metastable states of water. However, despite the active efforts in advancement and extension of knowledge on physical chemistry of water at negative temperatures, a number of problems concerned with fundamental properties of various water states have not yet been clarified [1–3]. Experimental study of metastable states meets difficulties of their reproduction and conservation under laboratory conditions. Conventional methods for studying of ordinary water knowingly stable at positive tem-

peratures appear to be inapplicable in this case. Interpretation of experimental results by no means always takes into account the features in the molecular structure of a modification under study.

The literature contains information on the following forms of H_2O existence in a liquid state at $T < 0°C$.

(i) Ordinary natural water with a density of ~ 1 g·cm^{-3} at 0°C, which, for brevity, let us call water-1. It is metastable with respect to transition into crystalline ice I. In the liquid state at negative temperatures or in the form of the so-called supercooled water, water-1 occurs in nature, in particular, in clouds and rainfalls (where it is most often confused with A-water described below). The experimentally determined lower limit of its physical existence is about −39°C [2].

(ii) A modification called amorphous water was obtained in many laboratory experiments as a solid

or viscous vitreous product of vapor condensation on substrates at temperatures of 100–150 K [1–3]. Its study at higher temperatures is hampered by the transition into a fluid state simultaneously with a sharp increase in the probability of spontaneous crystallization. The author of this paper detected stable existence of liquid-droplet amorphous water (A-water) in natural atmospheric clouds and measured some its properties [4–6].

(iii) A modification detected and studied in the 1960s by a team headed by B.V. Deryagin and called water II [7]. It retains a liquid state down to a temperature of at least 180 K even in contact with crystalline ice, in contrast to previous forms.

(iv) Bound nonfreezing water contained in biological tissues [2].

In this paper, we discuss a number of new results concerned with the properties of the first two water modifications. The study in this direction was initiated by new data on the microphysical structure of clouds, required nontrivial physical interpretation. Based on the data obtained, general understanding of the nature and properties of the amorphous H_2O phase was improved.

2. Supercooled water

As is known [8, 9], ordinary liquid water with a density of $1\,g{\cdot}cm^{-3}$ (water-1) features not a totally ordered internal structure formed by intermolecular hydrogen bonds. A structure-sensitive analysis based on X-ray and electron diffractions and other methods detects geometrical similarity of the averaged short-range order of the water-1 structure with the 3D hexagonal lattice of natural crystalline ice I_h. The difference of water-1 from ice with its rigid structure is spatiotemporal chaotic incompleteness of the similar system of bonds, which imparts the fluidity to water. The probability of supercooled water-1 freezing with transformation into ice I_h rapidly increases as the temperature is lowered and as the volume increases. The latter factor allows water to exist in the nature in the form of small cloud droplets not freezing at low temperatures. However, differing from ice by the saturating par-

tial pressure of vapor, cloud water-1 is evaporated in the presence of a dispersed ice phase.

To explain some anomalies in the properties of water-1, it should be taken into account that hydrogen bonds substantially separate bound molecules in comparison with other bond types typical of simple liquids [9]. This is exactly why the density of water-1 with its partially realized potential hydrogen bonds is higher than the density of ice I_h whose structure realizes all four possible bonds per each molecule. The specific hydrogen bond concentration in water-1 is inversely proportional to the energy of thermal vibrations of molecules. As a result, as the temperature is lowered, on the one hand, the water-1 density ρ_w should increase due to a decrease in the amplitude of thermal vibrations of molecules; on the other hand, ρ_w should be lowered due to an increase in the hydrogen bond concentration. The known ρ_w maximum at 4°C is caused by the prevalence of the former and latter tendencies at higher or lower temperatures, respectively.

The experimental dependence $\rho_w(T)$ for water-1 in the range 0°C to −34°C shows a progressive decrease in its density as the temperature is lowered [2]. This dependence is shown in Fig. 1 for the dif-
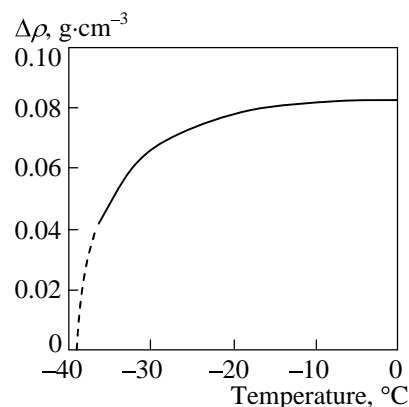

Figure 1. Temperature dependence of the difference between the liquid water-1 and ice I densities. The ice I density is set equal to $0.917\,g{\cdot}cm^{-3}$. The solid portion is plotted by the data of [2] and the dashed portion is extrapolation.

ference between of the density of liquid water and ice I, $\Delta\rho = \rho_w - \rho_i$, where $\rho_i = 0.917 \, g \cdot cm^{-3}$, and is extrapolated to the region of lower temperatures, based on the following considerations. The decrease in the water-1 density means its structure approach to the crystalline ice structure in the specific hydrogen bond concentration, hence, in the relative total volume of instant icelike clusters [10]. In this case, the probability of the stochastic formation of homogeneous ice nuclei with a zero nucleation energy threshold increases. At a critical temperature of water-1 existence, defined as a temperature of its fully homogeneous freezing, equal to −39°C [2], the water density should become equal to the ice density. This density equality means that the internal energy of water-1 becomes equal to the internal energy of ice at −39°C, and the latent energy of its freezing vanishes.

The latter circumstance was not reflected in reference values of the temperature dependence of the latent heat L_f of water freezing (for example, [11]). At $T > -30°C$, these values are derived from linear approximation of experimental data and from L_f extrapolation for lower temperatures. Assuming that $L_f(T)$ is proportional to the difference $\rho_w(T) - \rho_i$ to a first approximation, let us select such a proportionality factor that the obtained relation would be as much as possible close to the reference dependence at $T > -30°C$,

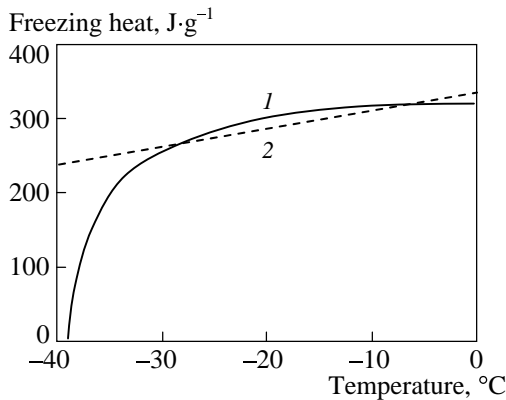$$L_f(T) = L_0 \frac{\rho_w(T) - \rho_i}{\rho_{w0} - \rho_i}, \qquad (1)$$

where $L_0 \approx 316 \, J \cdot g^{-1}$ and $\rho_{w0} = 1 \, g \cdot cm^{-3}$. The ice density ρ_i is assumed to be temperature-independent. Figure 2 shows dependence (1) in comparison with the reference curve $L_f(T)$.

In what follows, we shall return to the water-1 freezing mechanism within the consideration of the general case of metastable water.

3. Low-temperature amorphous condensate

Many experiments showed that a product of condensation of pure water vapor on a substrate at temperatures of ~ 100 K is a solid glassy substance without any ordered internal structure in contrast to ice and water-1 [1–3]. This water form was called by various authors as amorphous condensate, amorphous ice, solid amorphous water, and others. Monographs [1, 2] contain detailed reviews of early laboratory studies of the low-temperature amorphous condensate; numerous later papers are reflected in the detailed review by Angell [3].

Here we briefly generalize the results concerned with macroscopic properties of amorphous water.

Laboratory experiments showed that the solid amorphous condensate transforms into a viscous consistence upon heating above 135 K. As the temperature increases, its viscosity is exponentially lowered and the probability of its spontaneous crystallization with transformation into cubic ice I_c and then into hexagonal ice I_h rapidly increases. The viscous state stability depends on a condensate substrate material and its purity. At 150–160 K, the amorphous condensate takes on fluidity and almost absolute instability; therefore, the problem of the liquid state of amorphous water was not posed at all. Instead, discussions are not discontinued on the existence of a continuous intermediate state between supercooled water-1 and amorphous water. This state is expected to be related to both forms, while empirical searches for it still remain ineffective. Artificial matching of the temperature dependences of some characteristics of both forms, pro-

Figure 2. Conceptual (*1*) and reference (*2*) models of the temperature dependence of the specific latent energy of water-1 freezing.

posed in [1], which as if reflects properties of the hypothetical intermediate state, seems unjustified at least due to the strong dissimilarity of these dependences.

The concepts of such fundamental physical characteristics of the amorphous condensate as the density, evaporation and crystallization heats, and others, also yet have not gained certain completeness.

Most numerous estimations of the condensate density was based on its volume change during crystallization. Segregation of amorphous water on low-density ($0.94–1\,g\cdot cm^{-3}$) and high-density ($1.2–1.5\,g\cdot cm^{-3}$) waters was proposed in [3]. However, the proposed explanations of this and similar results are ambiguous. In what follows, we shall return to this problem.

In 1970, Delsemme and Wenger [12] reported on the determination of the solid condensate density at $T \approx 100\,K$ by measuring the geometrical volume of a sample and the mass of vapor expended for the condensate formation and released during evaporation. They obtained a value of $\rho = 2.32 \pm 0.17\,g\cdot cm^{-3}$. Despite the expressed doubts on the accuracy of these measurements [1], they seems free of principal errors, hence, are most reliable. Such a high density of the water condensate can be a consequence and indicator of the absence of hydrogen bonds in its structure, if and since hydrogen bonds keep H_2O molecules at a significantly longer distance than non-specific intermolecular bonds.

The latent heat of crystallization of the laboratory amorphous condensate was determined by the temperature jump at the crystallization front; a significant spread of estimates was observed, from 30 to $100\,kJ\cdot kg^{-1}$. Such low values typical of the "pre-ice" water-1 state (Fig. 2) are weakly consistent with its disordered molecular structure especially without hydrogen bonds.

4. Liquid water in natural ice-containing clouds (ICCs)

Aircraft measurements of microphysical characteristics of atmospheric clouds with negative temperatures were carried out in the late 1980s using a high-functionality and high-performance experi-mental system [13, 14] including the following instruments.

(i) **A particle phase/size analyzer (PPSA).** It carries out polarization and amplitude analysis of light pulses scattered at 90° by individual moving particles. Signals from crystals and spherical droplets are separated by the feature of strong light depolarization by crystals in contrast to droplets. The instrument separately determines concentrations of both particles, as well as the mixed spectrum of their sizes. Calibration by particle sizes includes calculation of the relative response for droplets by the Mie theory and its empirical referencing to the photoelectric converter using water-1 droplets (the refractive index is $n = 1.33$) of known size. Threshold values of the amplitude analyzer for water-1 droplet diameters, set at calibration, are from 30 to $180\,\mu m$. In special cases, it is possible to separate the spectra of droplet and crystal sizes in instrument readings [4, 5], thus, to perform the estimations described below.

(ii) **A large particle spectrometer (LPS).** It is based on the shadow method for measuring sizes of individual particles when they cross the planar light beam $\sim 100\,\mu m$ thick. This method allows a simple and accurate enough calculation of the calibration characteristic. The measurement range is from 0.2 to 6 mm.

(iii) **Liquid and total (liquid plus ice) water content meters (LWC and TWC meter, respectively).** Both instruments measure the electric current power P expended for evaporation of cloud water precipitated from a counterflow onto a hot ($\sim 90°C$) collector with receiving area S [15]. The streamlined shape of the IWO-Zh collector provides low sensitivity of the instrument to the ice phase. The basic calibration characteristic of the IWO is given by

$$W = P/uSL, \qquad (2)$$

where W is the water content (mass per unit air volume) of a given condensed phase, L is its specific evaporation heat, and u is the aircraft velocity.

(iv) **Transmissometric cloud transparency meter (RP).** The measured parameter is the luminous flux attenuation $T = \Phi/\Phi_0$ on an optical base of length

x between emitter and receiver. Then, according to Bouguer's law, the cloud extinction coefficient

$$E = x^{-1} \ln T^{-1} \qquad (3)$$

is determined.

The set of measured parameters allowed us to estimate a number of cloud characteristics not covered by direct measurements, as well as to correct the measured integral parameters W and E taking into account the dependence of the instrument readings on characteristic sizes of particles.

Statistically valid comprehensive measurements in the temperature range 0°C to −55°C detected the existence, along with supercooled water-1, cloud water with unusual properties which explain known anomalies in the properties of cold clouds [13, 16, 17].

Measurements with the LWC meter and PPSA instruments [13] showed that the liquid dispersed phase persists in ICCs even at temperatures below −40°C. It is contained mostly in large droplets of size tens and hundreds of micrometers, not typical of pure water (warm) clouds. At spatial variations in the cloud water content, the contents of liquid and ice phases, as a rule, positively correlate with each other.

All the above-listed properties of the liquid dispersed phase compose a complete set of necessary attributes of its condensation equilibrium with the ice phase in contrast to supercooled water-1. A comparison of the results of the determination of microphysical characteristics of clouds by various methods revealed differences of droplet water in ICCs from water-1 in other physical properties as well. The technique of the analysis of data is described in detail in [4, 5]; here we briefly outline it.

Significant systematic discrepancies between the W and E values measured and calculated by readings of the PPSA spectrometer were revealed according to its calibration for water-1 droplets. The calculated values multiply exceeded the measured ones. For the optical attenuation parameter E of a cloud, this disagreement was eliminated by using the PPSA data in the calculation, obtained according to the calibration characteristic for spherical particles with the refractive index $n =$

1.8–1.9. According to the estimation using the Lorenz–Lorentz formula [8],

$$\rho = \frac{1}{P(\lambda)} \frac{n^2 - 1}{n^2 + 2}, \qquad (4)$$

where $P(\lambda) = 0.206 \, \text{cm}^3 \cdot \text{g}^{-1}$ for yellow light (the invariant molecular characteristic of H_2O), the droplet material density should be from 2.0 to 2.3 $\text{g} \cdot \text{cm}^{-3}$. The use of these density values in the calculation of the liquid-droplet water content still does not eliminate the disagreement of calculated W with the data of measurements by the standard technique for water-1, i.e., at $L = 2580 \, \text{J} \cdot \text{g}^{-1}$ in Eq. (2). These values become equal when substituting $L = 550 \pm 90 \, \text{J} \cdot \text{g}^{-1}$ into Eq. (2). The total error of such determination of the evaporation heat of a liquid substance is $\sim 20\%$.

Since atmospheric clouds consist of chemically pure water, the described natural experiment reveals the existence of its liquid modification with a density more than $2 \, \text{g} \cdot \text{cm}^{-3}$ and an evaporation heat lower than that of water-1 by a factor of ~ 5. As previously [4, 5], we call this liquid modification as A-water.

The above conclusions are independently confirmed by a new interpretation of the natural optical glory phenomenon, described in detail in [18] and briefly in the next section.

5. Interpretation of the glory phenomenon

The glory is an optical phenomenon observed as a iridescent ring around the counter-Sun shadows of an observer at the upper boundary of a fog or cloud. In some cases, the glory ring is surrounded by one or several paler rings (Fig. 3). Although this phenomenon contains information on the existence and dispersity of the liquid-droplet fraction, it has not yet attracted close attention of researchers.

We succeeded to compile a rather complete description of the glory properties [18] from its description in the monograph by Minnaert [19], from our observations, and by analyzing more than 30 color photographs from an aircraft under vari-

Figure 3. Airplane view of the glory on a cloud. The glory ring center exactly coincides with the shadow projection of the camera objective. Photograph by A.V. Korolev.
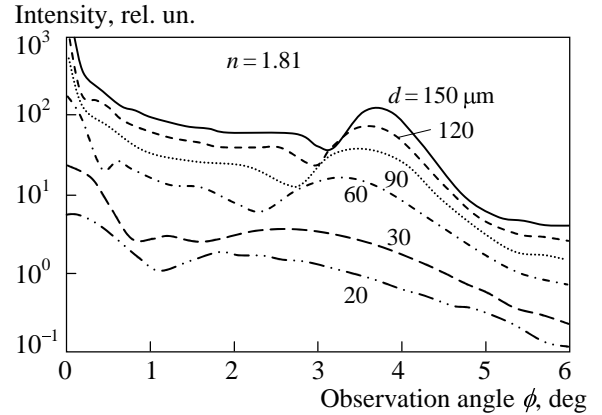

Figure 4. Scattering indicatrix fragments calculated by the Mie theory for yellow light ($\lambda = 0.58\,\mu m$) at the refractive index $n = 1.81$ providing formation of peaks in the range of visible angles of the natural glory at various sizes of monodisperse scattering spheres. The data are normalized to a unit cross section of a particle.

ous conditions. Typical properties of the glory are: (i) its formation in clouds with negative temperatures at the upper boundary; (ii) a red outer edge and strong positive polarization of light, as those of the rainbow; (iii) the range of measured angular radii of the basic ring is from 1.5° to 3.8° by the middle brightest yellow belt; (iv) the tendency of an increase in the brightness and color contrast with the angular size.

Currently, preference is given to the interpretation of the glory as a crown of light backscattering by water-1 droplets (the refractive index is $n = 1.33$). However, calculations by the Mie theory show that bow rings with the above-mentioned angular sizes can be formed in this case only in almost monodisperse clouds with droplet diameters from 8 to 12 μm, which are extremely improbable in the nature [11, 16, 17]. Moreover, they have properties not inherent to the actually observed glory, i.e., negative polarization and the inverse proportionality of the brightness to size.

Above we found a basis for interpretation of the glory as an effect of backscattering from spherical particles with refractive index different than $n = 1.33$. Indeed, the Mie theory reveals the existence of regular distinct peaks in the scattering indicatrix in the domain of observed glory angles only when the refractive index of scattering spheres is close to 1.8 and their diameters exceed ~20 μm (Fig. 4).

According to Fig. 4, the glory properties listed in Sec. 4 are explained by the dependences of the observation angle of the backscattering peak $\phi = \pi - \beta$, where β is the scattering angle, and its width on scattering droplet sizes. We note that the polarization factor is positive in each peak and follows its shape.

To make sure that the glory phenomenon is formed as a backscattering bow similar to the well known rainbow, let us compare the result obtained by the Mie theory and the geometrical theory of bow (for example, [20]). The expression for angles $\beta^{(k)}$ of bows of various orders k in relation to the refractive index n of scattering spheres can be written as

$$\beta^{(k)} = \left(k - 2j\right)\pi + 2\arcsin\frac{1}{n}\sqrt{\frac{\left(k+1\right)^2 - n^2}{\left(k+1\right)^2 - 1}}$$

$$-2\left(k+1\right)\arcsin\sqrt{\frac{\left(k+1\right)^2 - n^2}{\left(k+1\right)^2 - 1}}, \qquad (5)$$

where j is an integer, at which $0 \leq \beta^{(k)} \leq \pi$. Figure 5 shows the dependences of observation angles $\phi^{(k)} = \pi - \beta^{(k)}$ on n for backscattering bows of orders from 1 to 7. For the first-order bow, the same relation between angular sizes of the glory and the
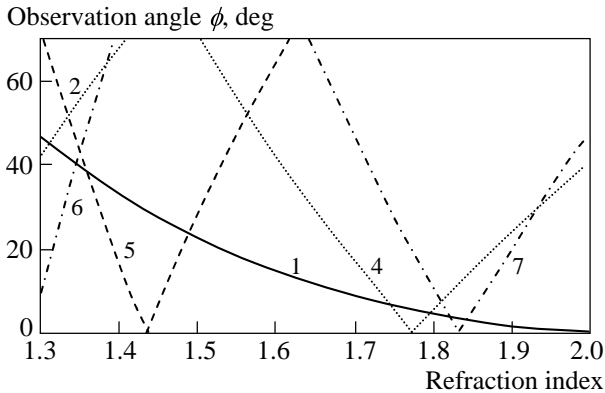
Observation angle ϕ, deg

Figure 5. Observation angles $\phi^{(k)}$ (calculated by the geometrical theory) of oppositely directed bows of various orders in relation to the refractive index of scattering spheres regardless to their sizes.

Observation angle ϕ, deg

Figure 6. Dependence of the first-order bow angle on the refractive index of spheres, calculated by the geometrical theory (upper curve) and by the Mie theory for sphere diameters of 30–150 μm at $\lambda = 0.58$ μm (yellow light).

order of values $n > 1.8$ is easily detected, as that obtained in the previous section, similarly to that as the calculated rainbow angle coincides with the actual one at $n = 1.33$.

The geometrical theory neglects the relative displacement of phases of converging beams forming the bow. The stronger the calculated bow angles deviate from peak maxima of the Mie theory, the higher the bow order is and the smaller the scattering sphere sizes. For both this reason and due to low bow intensities in the 4th and 7th orders, the glories adjacent to the definition domain in Fig. 5 are not detected in Fig. 4.

In Fig. 6, the right branch of the curve $\phi^{(1)}(n)$ from Fig. 5 is compared to a family of curves $\phi^{(1)}(n, d)$ obtained from curves calculated similarly to those in Fig. 4 at various n. It can be easily seen that the geometrical dependence $\phi^{(1)}(n)$ is a limit of the dependence $\phi^{(1)}(n, d)$ at $d \to \infty$. Figure 6 allows us to estimate the refractive index of cloud droplets, at which glories with average angular radii from $1.5°$ to $3.8°$ can be formed on droplets larger than 20 μm, as $1.81–1.82$. We recall that this estimate relates to yellow light; in red light, the corresponding n is $1.79–1.80$ [18].

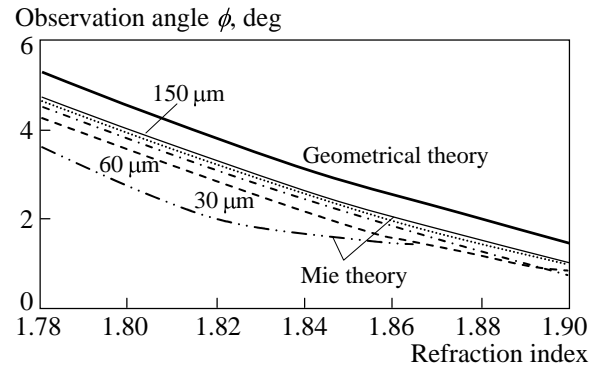As for weak additional rings in the general glory pattern (Fig. 3), their origin is explained in [18] by scattering of bow beams by ice crystals of prismatic shapes, whose peaks on the scattering indicatrix form the van Buijsen halo with a radius of $8°–9°$.

Thus, the glory phenomenon not only confirms the natural existence of the liquid form of water with specific properties, i.e., A-water, but also allows refinement of its properties. Using formula (4), the A-water density can be estimated as 2.1 g·cm^{-3}. Such a density should be inherent to amorphous water form whose molecular structure contains no hydrogen bonds [9].

Comparing the obtained characteristics of A-water with the data for the low-temperature condensate (Sec. 3), it is pertinent to put the question about possible causes of the detection of H_2O forms so differing in properties and attributed to the amorphous state in their properties. To answer this question, let us consider a general property of water in the metastable state, associated with its freezing (crystallization). Thereafter, we shall again return to specific properties of amorphous water.

6. Features of the mechanism of metastable water crystallization

When determining physical properties of amorphous water using its crystallization effects, one assumes conservation of mass of a freezing sam-

ple. The invalidity of this assumption becomes obvious, taking into account an inevitable release of the latent crystallization energy, compensated by energy expenditures for evaporation of A-water fraction from a sample. Taking into account the frontal nature of the freezing, the problem of the mass transfer mechanism and an evaporated water fraction appears to be not quite trivial.

It was found that all the above-mentioned metastable forms of water spontaneously transform into the same phase, i.e., ice I with a density of $\sim 0.92 \, \text{g·cm}^{-3}$. In all cases, the first-order phase transition occurs, which results in a jump separation of phase subspaces. Therefore, the crystallization mechanism of a continual sample is the phase interface, or crystallization front motion [1, 2]. At different phase densities on both front sides, as for water-1, and even more for A-water, a freezing particle should apparently change its shape or be destructed under internal stress. In fact, as demonstrated in many experiments, frozen water-1 droplets with various sizes remain spherical. For A-water, this effect is pronounced in the typical pattern of "riming" of cloud crystals by frozen droplets deposited on them (see, for example, [16]). In our opinion, the assumptions on the initial formation of an ice crust on the droplet surface or the folded surface of the freezing front [2] have no physical basis.

Another apparent paradox of the frontal crystallization follows from the conventional statement that the latent energy of indicated phase transition is released in pure thermal form. This heat should be released immediately at the front of the ice phase formation. In this case, the newly formed ice structure should be subjected to the initial temperature increment

$$\Delta T_0 = \frac{L_f}{c_{pi}}, \qquad (6)$$

where $c_{pi} \approx 2.0 \, \text{J·g}^{-1}\text{·K}^{-1}$ is the specific heat of ice. For water-1 with a temperature from −35°C to 0°C, determining L_f according to Fig. 2, we obtain ΔT_0 values from 100°C to 160°C. An even more impressive result is demonstrated by A-water, for which $L_f = L_i - L_e \approx 2300 \, \text{J·g}^{-1}$, where L_i is the evaporation

heat of ice. Here formula (2) yields $\Delta T_0 \approx 1150 \, \text{K}$. Thus, at the instant of its formation and during a finite time of temperature relaxation, ice should have a temperature much higher than its melting temperature, which rules out the possibility of its existence. This paradox inherent namely to frontal freezing has not yet been explained sufficiently.

Within the current concepts of the molecular structure of various water phases, both paradoxes have the following unified explanation [21]. Continuous motion of the interface during crystallization is caused by subsequent attachment of molecules from liquid to the crystal lattice of ice. Retained and newly formed hydrogen bonds are connecting links between both phases, providing their continuous bonding. The latter rules out the possibility of tangential slip of a liquid layer adjacent to the frontal surface. For this reason and due to its internal viscosity, a liquid trapped by the moving front is not deformed with respect to the solid ice base with the result that the newly formed ice phase retains the initial volume of the liquid phase. The ice density is smaller than the liquid density; therefore, A-water mass excess with respect to the ice structure is formed at the crystallization front. The energy released at the front is transferred to releasing molecules, converting into their kinetic energy.

The way how these unbound molecules leave the condensed medium can be partially clarified by an experiment with natural water freezing propagating from top to bottom in a vessel. In the case of such freezing, the lower vessel region, rather than the main region of ice formation, is subjected to deformation or destruction under internal pressure. This means that the forming ice not only retains the initial volume of liquid water, but is also impenetrable for emergence of excess molecules formed by the freezing front. However, the pressure increases in a closed liquid volume due to arrival of new molecules into it. This suggests that molecules rejected by the crystallization front can emerge to ambient air space only through an intermediate liquid medium.

Using an analogy with quite (film) boiling, the flow of forming free molecules in liquid can be

likened to molecular vapor outflow from a hot surface. Details of this phenomenon, still poorly studied, possibly include chain energy transfer from molecule to molecule. It is known that supercooled water can freeze at temperatures arbitrarily close to 0°C. This should mean that molecules rejected from the front leave a droplet not transferring to it any appreciable fraction of their energy. In other words, the adiabatic crystallization process is isothermal in space and time.

It follows from the above that the water fraction transforming into vapor during crystallization is

$$\frac{m_{\mathrm{v}}}{m_{\mathrm{w}}} = \frac{\rho_{\mathrm{w}} - \rho_{\mathrm{i}}}{\rho_{\mathrm{w}}}, \qquad (7)$$

where m_{w} and m_{v} are liquid water and vapor masses, respectively. For water-1, taking into account the dependences $\rho_{\mathrm{w}}(T)$ (Fig. 1), this fraction is 8.3 % at −1°C, 5.2 % at −35°C, and rapidly vanishes with decreasing temperature to −39°C. During crystallization of amorphous water with a density of ~2.1 g·cm⁻³, ~56 % of its mass transform into vapor. According to the simple calculation [21], the average velocity of molecules when crossing the liquid–vapor interface is tens meters per second.

We think that the above conclusions can be extended to the low-temperature amorphous condensate in the consistent state, which features metastability with respect to the transition into ice I. Indeed, during its crystallization, unknown gas release was sometimes observed [2], which, on reasonable considerations, can be only water vapor. The neglect of condensate loss for vapor formation at the phase transition naturally results in its underestimated density determined by a change in the condensate volume behind the crystallization front. The spread of the estimates of the amorphous condensate density, from the ice I density to ~1.5 g·cm⁻³ [3], is explained by the effect of secondary condensation of released vapor and its dependence on the degree of vapor supersaturation above a sample. The largest densities should be observed at the smallest closed volume containing a sample.

Known attempts to estimate the latent heat of amorphous condensate crystallization were based on an increase in the temperature of its sample during crystallization. In the light of the above data, we are inclined to that the observed temperature jump resulted from sample heating by the heat released upon secondary vapor condensation.

7. Properties of liquid amorphous water (A-water)

The above facts and considerations lead us to the conclusion that the low-temperature condensate obtained in many experiments [1–3], superdense ice [12], and A-water [4, 5], whose density is almost equal to that of superdense ice, belong to the same amorphous H_2O phase. Not only the high density of the amorphous modification counts in favor of that it has no intermolecular hydrogen bonds. The rectilinearity of each of O—H—O bonding chains and fixed angles between them [9] are related to the properties of hydrogen bonds between H_2O molecules. Therefore, the permanent existence of these chains rules out the existence of the completely disordered structure assumed in [3]. In our conclusion, the liquid form of amorphous water is a high-temperature melt, which is characteristic of materials with a glass structure. The existence of A-water in the form of droplets suspended in air provides better opportunities for more comprehensive study of the properties of the amorphous H_2O phase than laboratory conditions. Table 1 lists the physical properties of amorphous water, determined to date.

Let us consider the place of A-water in the phase hierarchy and phase transformations of H_2O, based on its properties and the features of the behavior in natural clouds and taking into account the known concepts of physical chemistry of the structure of matter [22].

Having the lowest enthalpy of condensation among condensed water phases, A-water can adiabatically nucleate only by condensation from vapor due to the second law of thermodynamics. Along with the above-determined condensation equilibrium of A-water with ordinary crystalline ice, these

Table 1. Experimentally determined physical parameters of the amorphous water phase.

Parameter	Conditions	Value	Notes
Softening temperature	$\eta = 10^{13}\,\text{P}$	$135 \pm 1\,\text{K}$	[1]
Temperature of yield stress	$\eta = 10^{9}\,\text{P}$	$\sim 150\,\text{K}$	[1]
Viscosity, η	$T > -55°\text{C}$	$< 10^{-2}\text{–}10^{-1}\,\text{P}$	[1]
Density	$T \approx -170°\text{C}$	2.32 ± 0.17 g·cm^{-3}	[12]
	$T = -30°\text{C}$	2.12 ± 0.15 g·cm^{-3}	[2,3]
Specific evaporation heat	$T = -30°\text{C}$	$550\,\text{J·g}^{-1} \pm 20\,\%$	[2]
Specific latent crystallization heat	$T = -30°\text{C}$	$2290\,\text{J·g}^{-1} \pm 5\,\%$	[2,4]
Refractive index		$1.81\text{–}1.82$	[2,5]
Partial pressure of saturated vapor	$T < 0°\text{C}$	It is identical to the values for ice I	[2]

[1] Extrapolation of the experimental data of [2].
[2] The data obtained for the liquid-droplet fraction in ICCs [4, 5].
[3] The value is derived from the refractive index by the Lorenz–Lorentz formula [8].
[4] The difference between the ice I and A-water evaporation heats.
[5] The value for yellow light, calculated by the glory angular size.

properties can be crucial ones to understand the role of the amorphous phase in the cloud ice genesis.

Indeed, this equilibrium means the identity of internal structures of free (droplet) A-water and the experimentally detected film enveloping the surface of ice particles and exhibiting properties of liquid [23]. Thus, the Fletcher assumption [24] about the non-hydrogen-bonded molecular structure of this intermediate layer is confirmed. The existence of this layer is a result of hydrogen bond breaking at the boundary of the ice structure itself. Unused bonds induce a surface electric charge that attracts free polar H_2O molecules. These molecules are concentrated as an amorphous condensate film oriented so that their total electric field would neutralize the field of the ice surface charge. The detected increase in the film thickness with the temperature compensates for violation of the ordered orientation of molecules due to their thermal motion. The transition layer of the amorphous condensate forms an energetically and structurally optimum intermediate medium for ice mass exchange with ambient vapor during its condensation and evaporation.

The fact that the transition layer consisting of A-water exists at the ice–vapor interface leads to the conclusion that A-water is a substance of an intermediate phase jump during condensation ice formation according to Ostwald's step rule. This rule establishes that "in any irreversible transition, the state least stable and most close to the initial state in free energy initially arises rather than the most stable state with the lowest free energy" [22]. The properties and behavior of A-water exactly correspond to the definition of the intermediate phase step in the process, where initial and final water states are water vapor and crystalline ice, respectively. The independent existence of A-water in the form of cloud droplets reflects the capability of the intermediate (according to Ostwald) phase to retain a metastable state. This means that only droplets with embedded heterogeneous crystallization centers (in the composition of condensation nuclei or of the contact origin) transform into ice. Therefore, the stability of amorphous water in natural clouds, in contrast to laboratory conditions, is provided by the incommensurately lower probability that a crystallization center exists in a mi-

croscopic condensation nucleus of each droplet in comparison with a laboratory substrate.

The physical nature of atmospheric condensation nuclei of A-water (CNAW) is related to the following anomaly. Typical of the atmosphere are layers (for example, under the bases of clouds of supercooled water-1) in which the relative humidity corresponds to undersaturation relative to water-1 and supersaturation relative to crystalline ice and A-water. Nevertheless, there is no cloud formation. Thus, active CNAW are absent in atmospheric air in the general case. More clarity in the CNAW formation is provided by such experimental facts as the ice crystal formation instead of a freshly evaporated droplet of supercooled water-1 [25] and the typical existence of small ($<20\,\mu m$) ice particles in clouds consisting of water-1 according to all other data [26, 27]. From this it follows that natural CNAW are, as a rule, of secondary origin, at least at $T>-39°C$, as a product of "drying" reactivation of water-1 condensation nuclei. At lower temperatures, the physics of their formation remains unclear.

We considered the A-water properties at negative temperatures. At positive temperatures, the partial pressure of saturated vapor above A-water, according to a smooth extrapolation of its temperature dependence for ice [11], becomes higher than above water-1. For $T>0°C$, this means that the equilibrium existence of A-water droplets suspended in the natural air medium containing water-1 condensation nuclei or droplets becomes problematic, since stable A-water saturation cannot be achieved in this medium.

At the same time, the existence of A-water at positive temperatures can be easily ascertained by observing its suspension in water-1, which is possible due to the difference of refractive indices and mutual insolubility of the two water modifications. When observing ice-melt water in a transparent vessel under strong lateral illumination during ice thawing, one can see transparent film pieces exfoliated from ice and decaying into smaller insoluble fragments as an attribute of fresh enough ice-melt water (Fig. 7). The fact that the shape of A-water droplets suspended in water-1 is far from spherical

Figure 7. It is easy to observe suspended insoluble impurity of A-water in ice water-1 under bright lateral illumination. The shape of impurity particles differs from that of spherical particles; in other respects, they behave as it consisting of a liquid heavier than water-1.

and their sizes depend on water mineralization still requires explanation. Sufficiently large particles sink with an appreciable velocity; some of them can coalesce with others, thus demonstrating their liquid state. At the vessel bottom, they coalesce into a liquid layer capable to transform again into a disperse admixture when water mixed.

8. Conclusion

The goal of this study was to complement incomplete current information on metastable liquid forms of water at negative temperatures. The statement and solution of this problem were initiated by the study of the microphysical structure of cold atmospheric clouds, which offered unique opportunities for studying two alternative H_2O states, i.e., supercooled ordinary water (water-1) and liquid amorphous water (A-water), in the interaction with each other and with ice. The observation results allowed us to independently determine char-

acteristics of A-water and to conclude that its molecular structure is non-hydrogen-bonded.

Quite distinct insight into the structure of various H_2O phases allowed us to correct the empirical temperature dependence of the latent heat of water-1 freezing, as well as to propose an explanation of the molecular crystallization mechanism for both metastable forms. We came to the conclusion that ice formed during crystallizations of metastable water retains its volume rather than mass as is conventional. The released energy of the phase transition is converted into the kinetic energy of free molecules released in this case. These and attendant effects were disregarded in attempts to determine the density and crystallization heat of a laboratory low-temperature condensate by a change in its volume and temperature after the transition into crystalline ice. These attempts gave rise to the widely accepted version about the existence of various modifications of amorphous water. Our results and conclusions contradict this version. We came to the conclusion that amorphous water under all conditions and states of its observation, from a low-temperature solid condensate to liquid at positive (centigrade) temperatures, belong to the same independent H_2O phase.

Within a critical generalization of known experimental results, we described main physical properties of the amorphous H_2O phase. At temperatures below $135\,K$, it is in a solid vitreous state. Upon heating above this temperature (softening point), it becomes consistent, i.e., from semisolid to viscous one; at $150–160\,K$, it takes on the fluidity, i.e., transforms into a liquid state. The amorphous water density is estimated as $2.3\pm0.2\,\text{g·cm}^{-3}$ at $\sim100\,K$ and $2.1\,\text{g·cm}^{-3}$ at $243\,K$. The refraction index in yellow light, determined using the natural glory phenomenon in clouds, is $1.81–1.82$. The evaporation heat at $243\,K$ is close to $550\,\text{J·g}^{-1}$. The saturating partial pressure of water vapor is the same as above ordinary crystalline ice I. The characteristics and behavior of amorphous water exhibit features of that, namely it is a polymorphic substance of the intermediate jump (according to Ostwald) in the vapor–ice phase transition. At the

same time, this substance can be retained in the metastable state.

The necessity and importance of further study of amorphous water are dictated by that it is very abundant in the nature. For example, its total content in clouds of the Earth's atmosphere is estimated as $10^{10}–10^{11}$ tons. It is also not improbable that amorphous water is incorporated in the disperse composition of cloud formations of other planets. A-water is contained in ice-melt water of various origins in the form of suspended microadmixture. Apparently, namely its existence imparts especially active biological and chemical properties to ice-melt water.

References

1. Skripov V.P. and Koverda V.P. Spontaneous Crystallization of Supercooled Liquids. Moscow: Nauka, 1984 [in Russian].
2. Water, a Comprehensive Treatise. Ed. F. Franks. N.Y.: Plenum, 1982.
3. Angell C.A. *Ann. Rev. Phys. Chem.* 2004, **55**, 559.
4. Nevzorov A.N. Proc. 11th Int. Conf. on Clouds and Precipitation. Montreal, 1992, p. 270.
5. Nevzorov A.N. *Meteorologiya i Gidrologiya* 1993, No. 1, 55 (*Meteorol. Hydrol.*).
6. Nevzorov A.N. Proc. 13th Int. Conf. on Clouds and Precipitation. Reno, Nevada, USA, 2000, p. 728.
7. Deryagin B.V. and Churaev N.V. New Properties of Liquids. Moscow: Nauka, 1971 [in Russian].
8. Eisenberg D. and Kauzmann W. The Structure and Properties of Water. Oxford: Oxford Univ., 1969.
9. Zatsepina G.N. Physical Properties and Structure of Water. Moscow: Lomonosov State Univ., 1998 [in Russian].
10. Pershin S.M. *Opt. Spectrosc.* 2003, **95**(4), 585.
11. Clouds and Cloudy Atmosphere. Handbook. Eds. I.P. Mazin and A.Kh. Khrgian. Leningrad: Gidrometeoizdat, 1989 [in Russian].
12. Delsemme A.H. and Wenger A. *Science* 1970, **167**, 44.
13. Nevzorov A.N. and Shugaev V.F. *Meteorologiya i Gidrologiya* 1992, No. 8, 52 (*Meteorol. Hydrol.*).
14. Nevzorov A.N. Proc. WMO Workshop on Measurements of Cloud Properties for Forecasts of Weather and Climate. Mexico City, 1997, p. 173.

15. Korolev A.V., Strapp J.W., Isaac G.A., and Nevzorov A.N. *J. Atm. Oceanic Techn*. 1998, **15**(6), 1495.
16. Pruppacher H.R. and Klett J.D. Microphysics of Clouds and Precipitation. Dordrecht: Reidel, 1978.
17. Mazin I.P. and Shtemer S.M. Clouds, Structure, and Physics of Formation. Leningrad: Gidrometeoizdat, 1983 [in Russian].
18. Nevzorov A.N. *Atmos. Res*. 2006 [in print].
19. Minnaert M.G.J. Light and Color in Nature. N.Y.: Springer, 1993.
20. Shifrin K.S. Introduction into Ocean Optics. Leningrad: Gidrometeoizdat, 1983 [in Russian].
21. Nevzorov A.N. *Izv. Akad. Nauk. Fiz. Atmos. Okeana* 2006 (*Izv. Atmos. Oceanic Phys.*) [in print].
22. Urusov V.S. Theoretical Crystal Chemistry. Moscow: Lomonosov State Univ., 1987 [in Russian].
23. Jellinek H.H.G. *J. Colloid Interface Sci*. 1967, **25** (2), 192.
24. Fletcher N.H. The Chemical Physics of Ice. Cambridge: Cambridge Univ., 1970.
25. Rosinski J. and Morgan G. *J. Aerosol Sci*. 1991, **22** (2), 123.
26. Nevzorov A.N. and Shugaev V.F. *Meteorologiya i Gidrologiya* 1992, No. 1, 84 (*Meteorol. Hydrol.*).
27. Nevzorov A.N. Proc. 12th Int. Conf. on Clouds and Precipitation. Zurich, 1996, p. 124.